Clays and Clay Minerals, Vol. 61, No. 3, 218–230, 2013.

STRUCTURE DETERMINATION OF TRIMETHYLSULFOXONIUM-EXCHANGED VERMICULITE

CANDICE A. JOHNS[1], RUBÉN MARTOS-VILLA[2], STEPHEN GUGGENHEIM[1,*], AND C. IGNACIO SAINZ-DÍAZ[3]

[1] Department of Earth and Environmental Sciences, University of Illinois at Chicago, 845 W. Taylor St., mc 186, Chicago, Illinois 60607, USA

[2] Facultad de Ciencias del Mar y Ambientales, Universidad de Cádiz, Av. República Saharaui s/n, 11510, Puerto Real, Spain

[3] Instituto Andaluz de Ciencias de la Tierra, CSIC-Universidad de Granada, Av. De las Palmeras, 4, 18100, Armilla, Granada, Spain

Abstract—The structure of trimethylsulfoxonium-exchanged vermiculite has been examined to compare it with other onium-exchanged structures, such as tetramethylammonium- and tetramethylphosphonium-exchanged vermiculite. The three organic cations are tetrahedral in shape, but trimethylsulfoxonium [$(CH_3)_3SO^+$] has an oxygen atom replacing a methyl group at one apex. This study describes the effect this substitution and the larger S atom have on the site location in the interlayer and the effect on the vermiculite 2:1 layer. These clay minerals may be commercially useful as adsorbents.

Na-exchanged crystals of vermiculite from Santa Olalla, Spain, were intercalated with trimethylsulfoxonium [$Me_3SO^+ = (CH_3)_3SO^+$] molecules by refluxing in an aqueous 0.25 M trimethylsulfoxonium iodide solution at 80ºC for 14 days. The resulting Me_3SO^+-exchanged vermiculite crystals were studied by single-crystal, X-ray diffraction methods and by computer modeling (density functional theory). Cell parameters are a = 5.349(2), b = 9.270(3), c = 13.825(8) Å, and β = 97.40(4)º, the space group is $C2/m$, and the polytype is 1M. Refinement results (R = 0.073, wR = 0.080) show that in the average structure of $C2/m$, the S atoms of the Me_3SO^+ molecules form two partially occupied planes [2.066(2) Å from each basal oxygen plane] between the 2:1 layers, and the S atoms show considerable positional disorder. The O atom of the Me_3SO^+ molecule occurs in the central plane of the interlayer, as far away from each 2:1 layer as possible. In projection down the c* axis, the Me_3SO^+ molecule resides within the center of the silicate rings from each adjacent 2:1 layer. In the ideal (static) model of the Me_3SO^+-exchanged vermiculite structure, the Me_3SO^+ molecule is oriented such that two methyl groups point toward charge-deficient bridging oxygen atoms of the basal plane; thus, the organic pillars charge compensate the bridging oxygen atoms of the 2:1 layer that are charge deficient. In projection, the oxygen atom of the Me_3SO^+ molecule projects over a tetrahedron containing Si. Computer modeling showed that if H_2O is not included in the model, the Me_3SO^+ molecule (S and O atoms) is in the center of the interlayer, but with the addition of randomly placed H_2O, two partially occupied planes similar to the X-ray derived model are formed.

Key Words—Computational Modeling, Organoclay, Trimethylsulfoxonium-exchanged Vermiculite, Vermiculite, X-ray Structure Determination.

INTRODUCTION

Pillared clays were originally defined as containing small, organic cations that hold the silicate layers apart, allowing for an accessible interlayer region for additional intercalation (Barrer, 1984; see also Guggenheim, 2013, for an updated definition). The pillaring organic cation is required to charge compensate the net negative charge on the silicate layer. Pillared clays are commonly derived from swelling clays, smectite, and vermiculite, and result in a fixed or nearly fixed layer-to-layer distance. Two potentially important properties for commercial use are: (1) depending primarily on the size and spacing of the pillar in the interlayer and the presence of adsorbed H_2O, a pillared clay may accept additional (sorbate) molecules selectively, based on size (*e.g.* Barrer, 1989; Lee *et al.*, 1990); and (2) these sorbates may be uncharged, polar, or non-polar molecules (e.g. Barrer and Millington, 1967; Barrer and Perry, 1961), presumably because of the van der Waals interactions provided by the pillaring organic cation. Thus, pillared clays are organophilic, whereas the original non-pillared clay may not be.

To understand the pillaring system in swelling clays better, single-crystal, X-ray structure determinations were made using a well crystallized and homogenous vermiculite sample. Onium-pillared structures included exchanges with tetramethylammonium (TMA^+) (Vahedi-Faridi and Guggenheim, 1997), tetramethylphosphonium (TMP^+) (Vahedi-Faridi and Guggenheim, 1999a), and monomethylammonium (MMA^+) and dimethylammonium (DMA^+) (Vahedi-Faridi and Guggenheim, 1999b). Two structural series are provided by these substitutions, with one series involving systematic addition of pillar complexity (MMA, DMA, and TMA pillars) to the vermiculite substrate. This series not only showed that interlayer sites were positioned much differently for the various pillars, but showed also that

* E-mail address of corresponding author:
xtal@uic.edu
DOI: 10.1346/CCMN.2013.0610305

the 2:1 layer was affected by the type of pillar present, with systematic differences in tetrahedral and octahedral bond lengths and angles. The other series, TMA- *vs*. TMP-exchanged vermiculite, involved a variation in pillar size (and charge density) for pillars with tetrahedral geometry. This series showed that size and charge density influences how the pillar may satisfy the net negative charge on the 2:1 layer, with the smaller cation (TMA) positioning itself near the center of the silicate ring of the 2:1 layer and the larger cation (TMP) associating with individual basal oxygen atoms.

The present study continues with a series approach. Trimethylsulfoxonium [$(CH_3)_3SO^+$, simplified to Me_3SO^+] is an organic cation of tetrahedral shape, but unlike TMA or TMP, it contains an oxygen atom at one of the tetrahedral apices around the centrally located sulfur atom. Thus, a change in the charge distribution is observed about the central cation. Therefore, the influence of this charge variation on the Me_3SO^+ cation and how it affects the site location in the interlayer can be evaluated and compared to the TMA- and the TMP-exchanged forms.

EXPERIMENTAL AND RESULTS

Sample and preparation

Vermiculite from Santa Olalla, Spain, was used. The structural formula determined after Ca intercalation and ignition is $Ca^{2+}_{0.85}(Mg_{5.05}Ti_{0.03}Mn_{0.01}Fe^{3+}_{0.58}Al_{0.28})(Si_{5.48}Al_{2.52})O_{22}$ (Norrish, 1973). Sections were cut to ~0.7 mm × 0.7 mm × 0.1 mm from the same crystal used by Vahedi-Faridi and Guggenheim (1997, 1999a, 1999b). Untreated crystals show that 0*kl*, $k \neq 3n$ (n = integer) reflections are streaked along the [001]* direction, indicating lack of three-dimensional periodicity and stacking disorder. One hundred crystals were Na-exchanged for 8 days in an aqueous 1 M NaCl solution at 80ºC. The solution was refreshed every 2 days. After exchange, the crystals were removed, rinsed three times in deionized water, and air dried for 24 h. Na exchange was monitored periodically using a Siemens D-5000 powder X-ray diffractometer with CuKα radiation. Na exchange resulted in a d_{001} value of ~14.7 Å. The purpose of the Na exchange was to increase the layer-to-layer distance to allow more rapid exchange with the large organo-cation.

The Na-exchanged crystals were refluxed in an aqueous 0.25 M trimethylsulfoxonium (Me_3SO^+) iodide solution at 80ºC for 14 days. The solution was refreshed every four days. Crystals were removed, rinsed three times in deionized water, and air dried for 24 h before examination on the powder X-ray diffractometer. A spacing of 13.47 Å was observed for the d_{001} reflection. Examination of 100 crystals showed that ~17% of the crystals were twinned, 20% of the crystals were very thin owing to cleavage along 001 during the exchange, 45% of the crystals were split partially on the (001) plane, and 9% showed too much stacking disorder for a structure determination. Fewer than 9% of the crystals were considered to be of sufficient quality for structure refinement, and the best was chosen for additional study, which showed three-dimensional order after the organic treatment. The 0*kl* and *h*0*l* reflections showed that suitable crystals were monoclinic with the presence of $h + k = 2n$ reflections, which define a *C*-centered cell, and an apparent mirror plane and two-fold axis. Space-group symmetry of *C*2/*m* was assumed initially, and *Cm* and *C*2 symmetries were considered also. The polytype is 1*M*. The nominal composition after Norrish (1973) and assuming complete exchange is: $[(CH_3)_3SO^+]_{1.7}(Mg_{5.05}Ti_{0.03}Mn_{0.01}Fe^{3+}_{0.58}Al_{0.28})(Si_{5.48}Al_{2.52})O_{20}(OH)_2$.

Data collection and refinement

The crystal was placed on a Picker four-circle diffractometer equipped with a graphite monochromator using MoKα (Kα = 0.71069 Å) radiation. Unit-cell dimensions were refined from 17 reflections in eight octants (136 reflections total) and values obtained were a = 5.349(2), b = 9.270(3), c = 13.825(8) Å, and β = 97.40(4)º. A total of 1426 reflections were collected from $h = -7$ to 7, $k = -12$ to 0, and $l = -10$ to 10 from 2θ = 2 to 70º. A total of 73 reflections was removed owing to irregular peak shapes or owing to very high intensity, the latter being of the type $k = 3n$ reflections. Reflections were measured at a scan rate of 2θ = 1º/min with a 2º scan window adjusted as a function of 2θ, and a background-time count equal to one half the scan time. Three standard reflections were monitored approximately every 2 h to check electronic and temperature stability. Data were corrected for Lorentz polarization and absorption effects and symmetry averaged using a locally written program (*Fobs-P*). After symmetry averaging, 576 observations above 4σ were obtained. Absorption effects were determined empirically from psi scans around the [010] direction taken at psi intervals of 10º for 0*k*0 reflections at various values of 2θ. For comparison to Vahedi-Faridi and Guggenheim (1997), the refinement proceeded as described in that paper.

Starting atomic coordinates for the 2:1 layer were taken from Vahedi-Faridi and Guggenheim (1997) for TMA-exchanged vermiculite in *C*2/*m* symmetry, but adjusted for differences in the *c*-cell parameter for the two crystals. Initially, no atomic parameters were included for interlayer material. Initial site occupancies were determined from the chemical formula of Norrish (1973), which indicated substitution in the tetrahedral and octahedral sites. Atomic scattering factor curves for half-ionized atoms were determined using the *International Tables for X-ray Crystallography* (1965). Reflections were assigned unit weights and a single scale factor. The scale factor was allowed to vary at all stages of the refinement. All atomic coordinates, x, y, and z, were varied except those fixed by symmetry, which brought the residual index to R = 0.309 and wR = 0.313,

https://doi.org/10.1346/CCMN.2013.0610305 Published online by Cambridge University Press

where $R = \Sigma(||F_o|-|F_c||)/\Sigma|F_o|$, $wR = [\Sigma w\ (|F_o|-|F_c|)^2/\Sigma w|F_c|^2]^{1/2}$, F_o = observed structure factor amplitude, F_c = calculated structure factor amplitude, $w = 1.0$. The isotropic thermal displacement parameter, B, was then refined for each atom in the 2:1 layer, which decreased the R values to $R = 0.174$ and $wR = 0.196$. Then, x, y, z, and B values were refined together. Positive and negative electron-density peak locations were determined using a difference-Fourier map. A possible sulfur peak in the interlayer was identified at x, y, z fractional coordinates of 0.4570, 0.5000, 0.3945 with an electron density of 3.49 electrons/Å^3 (e$^-$/Å^3). Introduction of the sulfur atom produced $R = 0.146$ and $wR = 0.151$.

Additional difference-Fourier maps were made and a possible oxygen atom peak was identified at 0.6660, 0.5000, 0.4785 fractional coordinates with an electron density of 1.58 e$^-$/Å^3. This atom position was determined to be that of a Me_3SO^+ oxygen and after refinement the R values were reduced to $R = 0.134$ and $wR = 0.144$. A second possible Me_3SO^+ oxygen position at 0.5000, 0.3945, 0.5039 with electron density of 0.989 e$^-$/A^3 was located. Placement of this atom in the model gave an occupancy value of 0.05, did not decrease the R values, and this peak was excluded in the refinement. As the last phase of the refinement, isotropic thermal displacement parameters were refined anisotropically (in U_{ij}) to better define atomic shapes, but the Me_3SO^+ oxygen position did not produce physically meaningful results. An anisotropic refinement with the Me_3SO^+ oxygen atom defined isotropically and with all parameters refined together resulted in final residual-index values of $R = 0.073$ and $wR = 0.080$. A final difference-Fourier map was used to try to locate methyl groups of the Me_3SO^+ cation and the hydrogen of the OH group of the 2:1 layer. All peaks in the difference map were below the background of $3\sigma = 0.624$ e$^-$/Å^3. Final atomic coordinates, calculated bond lengths and angles, calculated structural parameters for *C*2/*m* symmetry, and a refinement summary are reported in Tables 1, 2, 3, and 4, respectively.

Attempts to refine a model in *Cm* and *C*2 symmetries were unsuccessful. Refinement of x, y, and z coordinates of the 2:1 layer for the *Cm* model, expanded with atom parameters for the reduction in symmetry, resulted in (isotropic refinement) R values of $R = 0.168$ and $wR = 0.177$ (compared to $R = 0.138$ and $wR = 0.150$ for *C*2/*m* symmetry for the isotropic refinement). Attempts to refine displacement parameters did not produce physically meaningful results for the apical oxygen atoms. The *Cm* model showed the existence of a two-fold axis in the 2:1 structure. The model was thus abandoned in favor of the C2/*m* model. In the *C*2 model, refinement of the x, y, and z coordinates as expanded for the additional atom parameters resulted in isotropic refinement R values of $R = 0.136$ and $wR = 0.146$, but the atoms could not be refined anisotropically. Because of the large number of additional varied parameters compared to the

Table 1. Atomic coordinates of Me_3SO^+-exchanged vermiculite in *C*2/*m* symmetry.

Site	x	y	z	frac	B	U (1,1)	U (2,2)	U (3,3)	U (1,2)	U (1,3)	U (2,3)
M(1)	0.5	0	0	0.253(3)*	1.85	0.0057(9)	0.0017(3)	0.0056(3)	0	0.0010(9)	0
M(2)	0	0.1689(3)	0	0.520(4)**	1.96	0.0068(6)	0.0019(2)	0.0059(2)	0	0.0019(6)	0
T	0.3993(3)	0.1666(2)	0.1993(2)	1	2.13	0.0066(4)	0.0018(2)	0.0067(2)	0.0001(5)	0.0031(4)	−0.0002(3)
O(1)	0.445(1)	0	0.2405(7)	0.5**	3.29	0.020(2)	0.0032(6)	0.0084(7)	0	0.002(2)	0
O(2)	0.1465(8)	0.2338(6)	0.2415(5)	1	3.35	0.014(1)	0.0057(5)	0.0085(5)	0.005(1)	0.004(1)	0.0000(8)
O(3)	0.3603(7)	0.1671(4)	0.0809(4)	1	2.11	0.009(1)	0.0027(4)	0.0057(4)	0.000(1)	0.001(1)	0.0000(6)
OH	0.360(1)	0.5	0.0771(6)	0.5**	1.98	0.005(1)	0.0021(6)	0.0061(6)	0	0.002(1)	0
S	0.464(5)	0.5	0.392(2)	0.175(7)**	11.13	0.10(1)	0.027(3)	0.016(2)	0	0.009(8)	0
O(4)	0.607(6)	0.447(3)	0.497(3)	0.16(1)	4.3(8)						

frac indicates refined value of site occupancy.
* indicates an atom located at the center of two symmetry operators where the true site occupancy value is the refined frac value multiplied by 4.
** indicates an atom located on a symmetry operator where the true site occupancy value is the refined frac value multiplied by 2.

https://doi.org/10.1346/CCMN.2013.0610305 Published online by Cambridge University Press

Table 2. Selected calculated bond lengths and angles for the *C*2/*m* refined model.

		Distance (Å)			Distance (Å)		Angle (°)
2:1 layer							About *T*
T	−O(1)	1.654(4)	O(1)	−O(2)′	2.691(5)		108.8(3)
	−O(2)′	1.655(5)		−O(2)	2.694(6)		108.6(3)
	−O(2)	1.662(5)		−O(3)	2.686(9)		110.1(4)
	−O(3)	1.623(6)	O(2)	−O(2)′	2.691(5)		108.4(3)
	Mean	1.649		−O(3)	2.698(8)		110.4(3)
			O(2)′	−O(3)	2.690(8)		110.2(3)
				Mean	2.692	Mean	109.4
			Shared				About *M*(1)
M(1)	−O(3) × 4	2.104(4)	O(3)	−O(3) × 2	2.847(7)		85.16
	−OH × 2	2.081(6)		−OH × 4	2.813(9)		884.45
	Mean	2.096			Mean 2.824		
			Unshared				
			O(3)	−O(3) × 2	3.099(6)		94.84
				−OH × 4	3.099(5)		95.55
					Mean 3.099		
			Shared				About *M*(2)
M(2)	−O(3) × 2	2.082(5)	O(3)	−O(3)	2.847(7)		86.28
	−O(3)′ × 2	2.100(4)		−O(3)′ × 2	2.843(7)		85.65
	−OH × 2	2.086(5)	OH	−O(3)′ × 2	2.813(9)		84.45
	Mean	2.089		−OH	2.75(1)		82.67
					Mean 2.82		
			Unshared				
			O(3)	−O(3)′ × 2	3.084(5)		95.03
				−OH × 2	3.083(5)		94.87
			OH	−O(3)′ × 2	3.086(4)		95.53
					Mean 3.084		

Me_3SO^+		Me_3SO^+-nearest 2:1 layer	
S−O(4)	1.63(5)	S−*T*	4.06(2)
		S−O(2)	3.52(2)
		S−O(2)′	3.24(2)
		S−O(3)	5.26(2)
		S−OH	4.32(3)
		S−*M*(1)	5.66(3)
		S−*M*(2)	5.67(3)

*C*2/*m* model and the inability to refine the *C*2 model successfully, the *C*2 model was abandoned also.

Computational methods

Calculation procedures. Quantum mechanical calculations of an isolated Me_3SO^+ molecule were performed using the Hartree-Fock approximation with the second-order Moeller-Plesset (MP2) method for describing the electron exchange correlation for all electrons. The molecular electronic structure was calculated with a triple-ζ basis set with polarization functions for all atoms including H atoms (MP2/6−311G** level) as implemented in the *Gaussian03* program (Frisch *et al.*, 2004). No geometry constraint was applied to the molecule, which was optimized fully using the Berny analytical gradient method. Normal vibration modes were calculated from the force-constant analysis to confirm the nature of the stationary points, which resulted in only positive eigenvalues for the minimum. The molecular structure of Me_3SO^+ as a gas produced S−O and S−C distances of 1.454 Å and 1.775 Å, respectively, with the O−S−C angle of 113.7º.

Ab initio total energy calculations of the periodic crystal model were performed using density functional theory (DFT) methods based on the numerical atomic orbital (NAO) methodology implemented in the *SIESTA* program (Soler *et al.*, 2002). The generalized gradient approximation (GGA) was used with the Perdew-Burke-Ernzerhof (PBEsol) parameterization of the exchange-correlation function optimized for solids (Perdew *et al.*, 2008). Core electrons were replaced by norm-conserving pseudopotentials (Troullier and Martins, 1991). Calculations were restricted to the Γ point in the irreducible wedge of the Brillouin zone. In all model

https://doi.org/10.1346/CCMN.2013.0610305 Published online by Cambridge University Press

Table 3. Calculated structural parameters for Me_3SO^+-exchanged vermiculite.

Parameter	Value
$\alpha(^o)$*	6.40
$\psi(^o)$**	59.68 (*M*1)
	59.57 (*M*2)
$\tau_{tet}(^o)^\dagger$	110.28
Sheet thickness‡	
Octahedral (Å)	2.116
Tetrahedral (Å)	2.202
Interlayer separation (Å)	7.099
$\beta_{ideal}(^o)^\S$	97.41
Cation distance to basal oxygen plane (Å)	2.073

* α (º) = ½[120 − mean $O_b-O_b-O_b$ angle]
** ψ (º) = $\cos^{-1}$[(oct. thickness)/(2(M−$O)_{ave}$)]
† τ_{tet} (º) = mean O_b-T-O_a
‡ Octahedral sheet thickness includes OH
§ β_{ideal}(E) = 180 − $\cos^{-1}$[a/3c]

structures, each atom was relaxed by conjugate gradient minimizations at constant volume. In *SIESTA*, the basis sets consist of strictly localized numerical atomic orbitals (NAOs) with a localization cut-off radius corresponding to an energy shift of 270 meV. The basis sets used here are double-Z polarized (DZP) following the perturbative polarization scheme. This approach was used successfully in previous calculations on phyllosilicates (Hernández-Laguna *et al.*, 2006).

A uniform mesh with certain plane-wave cut-off energy was used to represent the electron density, the local part of the pseudopotential, and the Hartree and exchange-correlation potentials. Calculations were performed with cut-off energy values of 150 Ry. These conditions are consistent with previous studies with phyllosilicates (Sainz-Díaz *et al.*, 2005).

Model development and the basic 2:1 layer. Model development involved defining each component of the phyllosilicate and then assembling these components. Analyses were made using increasingly complex assemblages. A periodic model of the crystal structure of vermiculite was generated from the experimental atomic coordinates and cell parameters given in Vahedi-Faridi and Guggenheim (1997). To create a supercell of a reasonable size for modeling, the structural formula of the vermiculite 2:1 layer was simplified to: $(Mg_{5.25}Al_{0.75})(Si_{5.5}Al_{2.5})O_{20}(OH)_4$ per unit cell, where the layer charge per unit cell is −1.75. Maximum separations between cation substitutions in the tetrahedral and octahedral sheets are used because these configurations are most stable (Sainz-Díaz *et al.*, 2003). Each model consisted of a supercell of $2\times2\times1$ vermiculite unit cells. To compensate the layer charge in this supercell, Me_3SO^+ cations, as optimized by quantum mechanical calculations (see above), were placed in the supercell to explore the different possible arrangements in the interlayer.

Models involving intercalated Me_3SO^+. The Me_3SO^+ molecule, initially optimized at the MP2/6-311G** level, was placed in the vermiculite crystal lattice based on the experimental X-ray diffraction (XRD) data and re-optimized using the DFT-*SIESTA* approach before intercalation. Seven Me_3SO^+ molecules are within the $2\times2\times1$ supercell of vermiculite, three of which are located within the upper-layer tetrahedral-ring cavity and four in the lower-layer, alternately choosing the tetrahedral-ring cavities with greatest local charge. One pair of cavities is without Me_3SO^+. In the optimization calculations of the dry (no H_2O) model, all Me_3SO^+ molecules are displaced to the center plane of the interlayer region, with the S and O atoms in the center of the interlayer and the methyl groups pointing to the basal oxygen atoms of the tetrahedral sheet (Figure 1).

Table 4. Summary of parameters.

Formula	$[(CH_3)_3SO^+]_{1.7}(Mg_{5.05}Ti_{0.03}Mn_{0.01}Fe^{3+}_{0.58}Al_{0.28})(Si_{5.48},Al_{2.52})O_{20}(OH)_2$
Z	1
Polytytpe	1M
CEC[1]	140 meq/100 g
Crystal size (mm)	~$0.7\times0.7\times0.1$
Cell parameters	a = 5.349(2), b = 9.270(3), c = 13.825(8) Å, and β = 97.40(4)º
Crystal system	monoclinic
Space group	$C2/m$
hkl range and theta	h = −7 to 7, k = −12 to 0, and l = −10 to 10 from 2θ = 2 to 70º
Number of reflections	total measured: 1426, independent: $I > 4\sigma$, 576
Absorption correction	empirical, *via* psi scan
R (on F)	= $\Sigma(\|\|F_o\|-\|F_c\|\|)/\Sigma\|F_o\|$ = 0.073
wR (on F)	=$[\Sigma w\ (\|F_o\|-\|F_c\|)^2/\Sigma w\|F_c\|^2]^{1/2}$ = 0.080
Largest difference peak	< 0.624 $e^-/Å^3$

[1] Measured on Mg-vermiculite, Santa Olalla, sample (Ruiz-Conde *et al.*, 1997).

https://doi.org/10.1346/CCMN.2013.0610305 Published online by Cambridge University Press

Models involving H_2O + Me_3SO^+. Different numbers of H_2O molecules were added to Me_3SO^+-vermiculite models in a disordered fashion. For example, the W3 model: three H_2O molecules are located in each cavity at the opposite site to each Me_3SO^+ (13.6 % w/w of total water content); W4: the same as W3, but adding four H_2O molecules per Me_3SO^+ (16.1% total water content); W5: adds five H_2O molecules per Me_3SO^+ (20.7% total water content). In each case, seven Me_3SO^+ molecules and eight pairs of tetrahedral-ring cavities are in each supercell, and the cavity pair without Me_3SO^+ is filled with five to ten H_2O molecules.

Geometry optimizations for the W3 models place Me_3SO^+ molecules at the center of the interlayer (Figure 1b). Density profiles of the S atom along the [001] direction show a maximum at 3.58 Å from the lower basal-oxygen plane of the tetrahedral sheet (Figure 2). However, density profiles of the O atom from Me_3SO^+ molecules shows two peaks, corresponding to different positions of Me_3SO^+ molecules in the interlayer (Figure 3). For the W4 model, Me_3SO^+ molecules are located closer to the basal-oxygen planes of the tetrahedral sheets (Figure 1c) than in the W3 model. Density profiles of S atoms show two peaks from Me_3SO^+ molecules at an average distance of 2.83 Å from the lower basal-oxygen plane and 3.10 Å from the upper plane (Figure 2c). Similar to the W3 model, O atoms of the Me_3SO^+ molecule form two separate planes (Figure 3c). For the W5 model, Me_3SO^+ molecules are located to form two planes in the interlayer (Figure 1d), but more separated from each other than in W4. The S atom has an average distance of 2.70 Å from the lower basal-oxygen plane and 2.16 Å from the upper plane (Figure 2d). Oxygen atoms of the Me_3SO^+ molecule form one plane in the center of the interlayer (Figure 3d).

DISCUSSION

Space-group determination and refinement

The determination of the symmetry to use in a least-squares refinement can be problematic. The problem is especially severe in Me_3SO^+-exchanged vermiculite

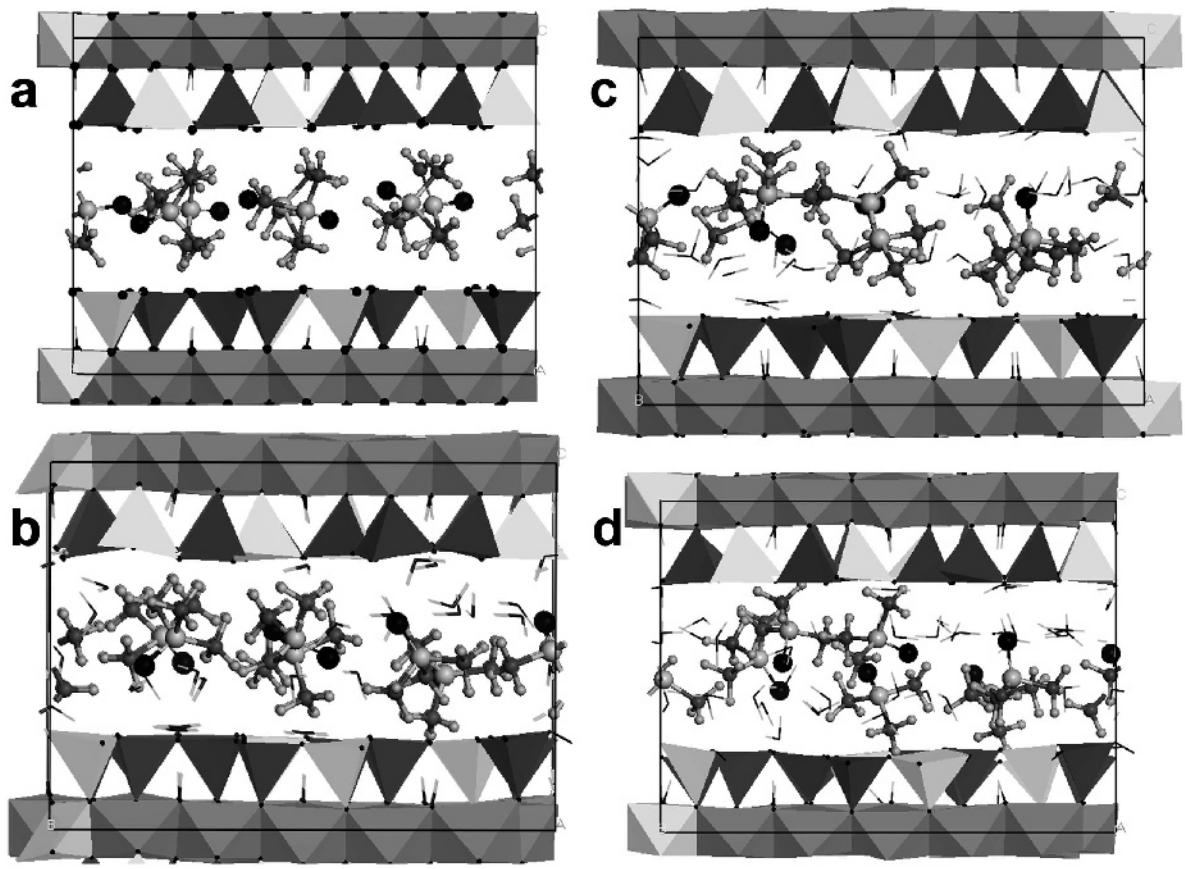

Figure 1. Optimized crystal structure of Me_3SO^+-exchanged vermiculite models: (a) vermiculite- model; (b) vermiculite-W3 model; (c) vermiculite-W4 model; (d) vermiculite-W5 model. Vermiculite 2:1 layers are represented as follows: Mg atoms are octahedral polygons, Al atoms are light-gray octahedral and tetrahedral polygons, and Si atoms are dark gray tetrahedral polygons. H and O atoms from water molecules are represented by light gray and black sticks, respectively. S, O, C, and H atoms from Me_3SO^+ molecules are represented by light gray, black, dark gray, and small light gray balls, respectively.

https://doi.org/10.1346/CCMN.2013.0610305 Published online by Cambridge University Press

where the majority of atoms (*e.g.* those in the 2:1 layer) show high symmetry (*i.e. C*2 and C*m*) and dominate the diffraction pattern, and where a relatively small number of atoms (*e.g.* Me_3SO^+) is present that may not follow the same symmetry. In addition, the Me_3SO^+ molecules show positional disorder and have relatively low electron density per site occupied, thereby making the determination of symmetry more difficult. One approach is to make trial refinements in lower symmetry using plausible subgroups, as was done here. For example, one possible subgroup symmetry, *Cm*, is plausible if the Me_3SO^+molecule occurs on the mirror plane, with this plane bisecting the central S atom and the O atom of the Me_3SO^+ molecule. This refinement was unsuccessful.

Single-crystal, XRD methods provide data on the average structure of the material studied, because the least-squares method involves atom-position information over all the unit cells in the crystal. Another possible subgroup symmetry, *C*2, is plausible on a statistical basis with the 2-fold axis relating two sites with

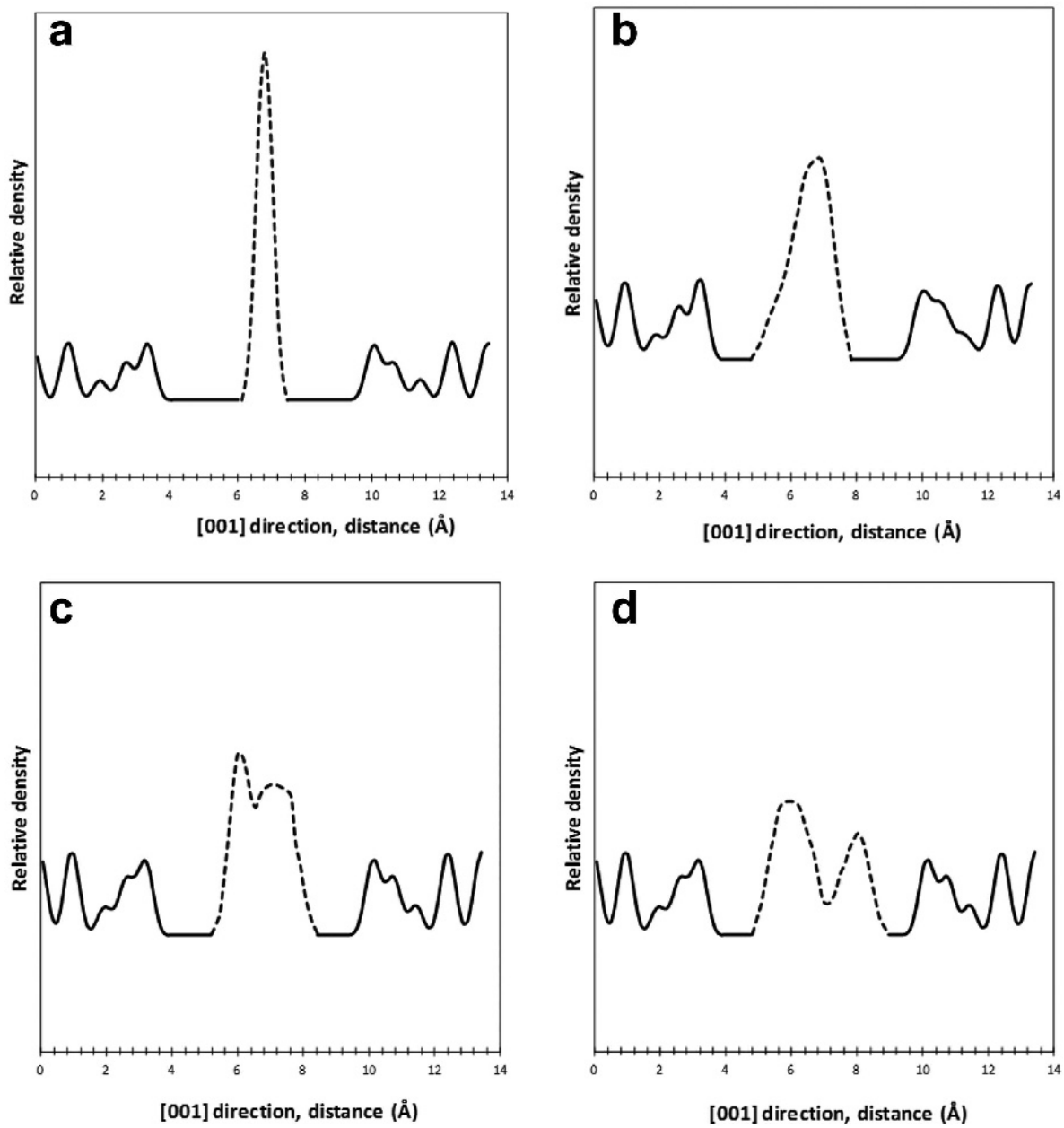

Figure 2. Electron density profiles along the *c* axis of the interlayer of vermiculite models: (a) vermiculite model; (b) vermiculite-W3 model; (c) vermiculite-W4 model; (d) vermiculite-W5 model. Dashed lines represent S atoms from molecules; black lines represent the 2:1 layer electron density of vermiculite.

https://doi.org/10.1346/CCMN.2013.0610305 Published online by Cambridge University Press

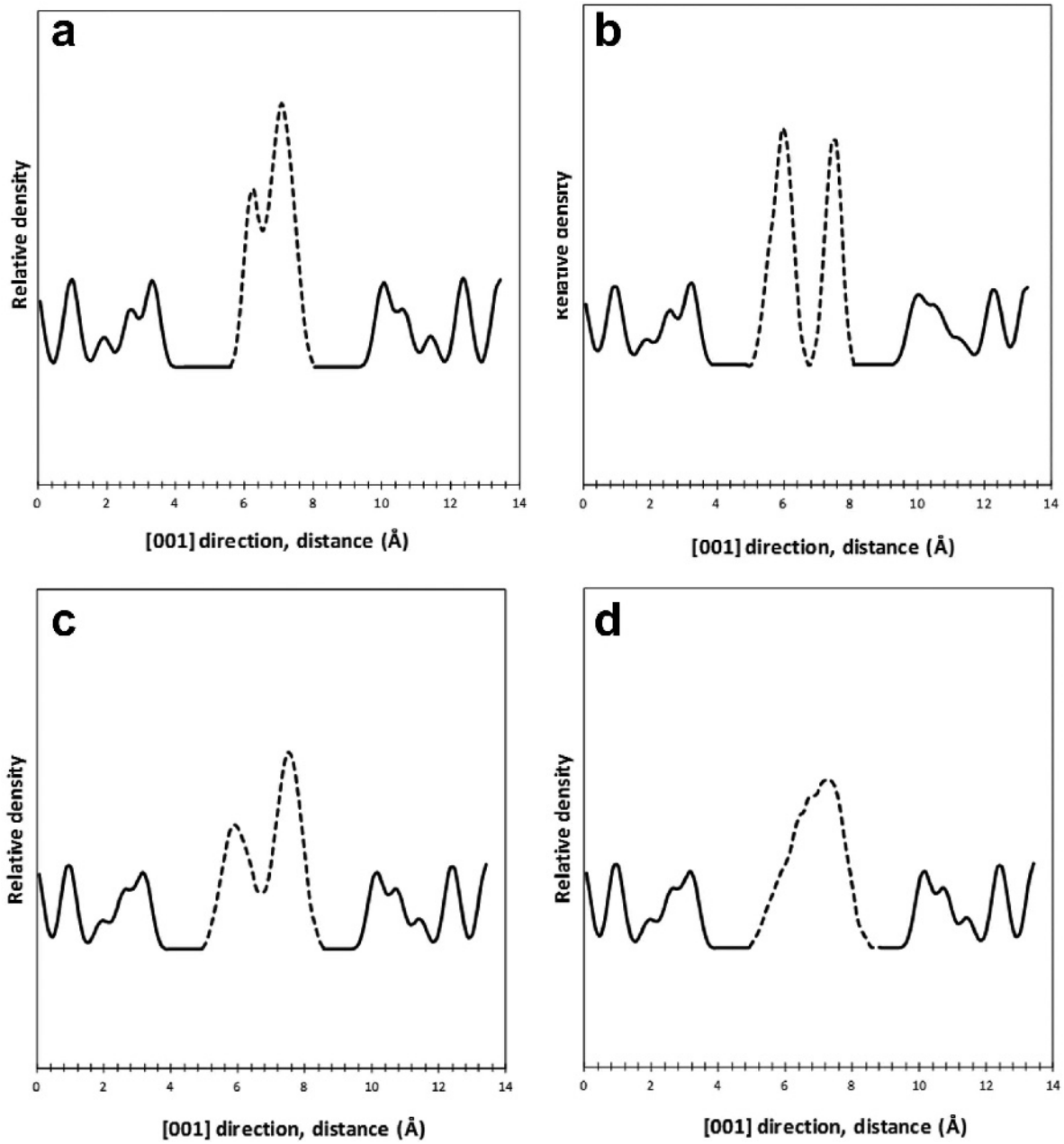

Figure 3. Electron density profiles along the *c* axis of the interlayer of vermiculite models: (a) vermiculite model; (b) vermiculite-W3 model; (c) vermiculite-W4 model; (d) vermiculite-W5 model. Dashed lines represent O atom from the molecules; black lines represent 2:1 layer electron density profiles of vermiculite.

Me_3SO^+molecules that are partially occupied in such a way that both sites are not occupied simultaneously. This refinement was also unsuccessful. Failure to obtain a successful refinement in *Cm* and *C*2 subgroup symmetries suggests that the parent space group of *C*2/*m* best describes the X-ray data. A third subgroup model, $C\bar{1}$, was not considered in detail and is considered to be very unlikely based on the results of the other subgroup models.

In space group *C*2/*m*, the resultant position for the sulfur atom (Table 1) shows a high isotropic displacement parameter near 11 Å^2. For inorganic crystal structures, a value this high may be an indication of a misplaced atom, but in this case there are several reasons why this may not be the case: (1) organic molecules often have high displacement factors relative to inorganic species (Stout and Jensen, 1968); (2) the residual *R* value dropped significantly when the S atom

https://doi.org/10.1346/CCMN.2013.0610305 Published online by Cambridge University Press

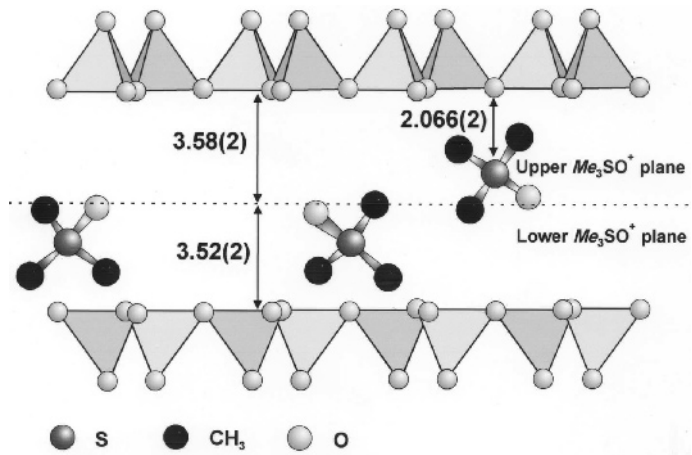

Figure 4. Diagram showing the Me_3SO^+ molecules in two distinct planes in the interlayer as projected down the [100]* direction. Various Me_3SO^+ orientations are shown. Sulfur-atom and oxygen-atom distances (Å) to the basal oxygen atom plane are given. Numbers in parentheses indicate estimated standard deviations, where 3.58(2) indicates 3.56 to 3.60 Å. The 2:1 layer is incomplete as shown.

was included in the refinement (wR = 0.196 to 0.151); (3) the high displacement parameter is probably indicative of the considerable positional disorder (see below) expected where electrostatic interactions exist between the interlayer molecule and substitutional disorder (Al *vs*. Si) within the silicate ring of the 2:1 layer; and (4) the S site location is crystallochemically reasonable.

The average interlayer structure and disordered H_2O

Because interlayer water molecules could not be located from the X-ray data, computer modeling was used to determine the effect of disordered H_2O on the position of the Me_3SO^+ molecule. Without H_2O present, models indicated that the Me_3SO^+ molecule would reside in a central plane between two adjacent 2:1 layers. This is the configuration found in the single-crystal X-ray refinement of TMA-exchanged fluorhectorite (Seidl and Breu, 2005). However, Vahedi and Guggenheim (1997), in TMA-exchanged experiments in water similar to the Me_3SO^+ sample preparation procedures used here, found that the Me_3SO^+ cation occurred in two planes in the interlayer, and the results were supported by the computational methods described by Martos-Villa *et al.* (2013).

Sulfur of the Me_3SO^+ molecule is offset by 0.160(4) Å from the center of the six-member ring of Si,Al tetrahedra of the 2:1 layer. The S is 2.066(2) Å from the basal-oxygen atom plane of each adjacent 2:1 layer; thus, Me_3SO^+ molecules are located in two planes in the interlayer (Figure 4). The planes are referred to as 'upper' and 'lower' Me_3SO^+ planes as labeled in Figure 4. The sulfur atom has an average distance of 4.06(2) Å from each tetrahedral cation of the nearest tetrahedral ring and 3.38(3) Å from each basal oxygen atom (O_b), nearest the plane in which the Me_3SO^+ resides (Figure 4). Three basal oxygen atoms (inner) are closer to the sulfur [S−O_b distance of 3.24(2) Å], and three (outer) are further away [S−O_b of 3.52(3) Å]. The S−O4 bond distance (where O4 is part of the Me_3SO^+ molecule) is 1.63(5) Å, as compared to 1.439(2) Å in trimethylsulfoxonium perchlorate (Kolinsky *et al.*, 1994). The short S−O bond distance in the trimethylsulfoxonium perchlorate structure is probably a consequence of repulsions between the oxygen atom of the Me_3SO^+ molecule and ClO_4^-.

The oxygen atom of each Me_3SO^+ molecule is located at the center of the interlayer, at 3.52(2) Å (lower Me_3SO^+ plane) or 3.58(2)Å (upper Me_3SO^+ plane) from the basal-oxygen plane of the tetrahedral sheet (Figure 4). Table 1 includes only one oxygen-atom position for the Me_3SO^+ group, but an electron-density map at the final stage of the refinement suggests considerable positional disorder around the sulfur atom for the oxygen atom, and the significance of this is discussed below for the ideal structure. Because the axis of the Me_3SO^+ tetrahedron is established by the S and O4 positions, methyl-group positions can be inferred. Possible methyl-group positions are discussed below. No H_2O molecules were found, but the possibility exists that they occur randomly in the interlayer because the crystal was exchanged in an aqueous solution and air dried. In the simulations, some water molecules are joined tightly to the tetrahedral O atom, forming strong hydrogen bonds of 1.45−1.70 Å to the basal O atoms and 1.48−1.79 Å to the H atom of the octahedral OH group. Hence, these strong interactions would make the release of water from the mineral particle more difficult. In addition, the interactions between water molecules and the Me_3SO^+ cations would make the release of H_2O from the interlayer even more difficult, and this is consistent with the standard hygroscopicity of the Me_3SO^+ halide salts.

https://doi.org/10.1346/CCMN.2013.0610305 Published online by Cambridge University Press

The 2:1 layer

Calculated structural parameters for the Me_3SO^+-exchanged vermiculite are defined and given in Table 3. These determined values are similar to those obtained for the 2:1 layer (*i.e.* sheet thicknesses, α, ψ, and τ_{tet}) for the other onium-exchanged vermiculites (*cf.* table 5 of Vahedi-Faridi and Guggenheim, 1999b). The most notable deviation is the tetrahedral rotation angle, α, which describes the in-plane rotation of adjacent tetrahedra around the silicate ring that results in a ditrigonal distortion of that ring. The α value in the Me_3SO^+-exchanged vermiculite is 6.4º (*cf.* TMA, 7.1º; TMP, 6.75º), consistent with the TMA molecule being positioned more deeply in the silicate ring than the Me_3SO^+ molecule (TMA, N to basal-plane distance = 1.91 Å; Me_3SO^+, S to basal-plane distance = 2.07Å). Differences in positioning occur because of the smaller size of TMA relative to the Me_3SO^+ molecule and the effects of an oxygen atom apex of the Me_3SO^+ molecule (see below). Thus, the TMA molecule can better attract first nearest neighbor basal oxygen atoms than the Me_3SO^+ molecule, to produce a greater α value. Because, on average, TMP-exchanged vermiculite has TMP molecules associated with each bridging basal oxygen atom, a direct comparison with Me_3SO^+ in Me_3SO^+-exchanged vermiculite is limited.

The ideal (static) interlayer structure

Three important aspects of the 2:1 layer in developing a static model for the interlayer include: (1) a ditrigonal silicate ring is formed; (2) ditrigonal rings in adjacent sheets across the interlayer superimpose (hereafter referred to as 'paired rings') when viewed down the [001]* direction, and (3) Al cations may randomly substitute for Si in the tetrahedral sites. Because the average unit cell apparently contains multiple Me_3SO^+ locations, a model must involve two S sites that occur near one another, although not necessarily occupied simultaneously. The S−S and O(4)−O(4) distances between adjacent Me_3SO^+ molecules are given in Table 5. The O(4)−O(4) distances shown in Table 5 are the minimum and maximum distances between neighboring oxygen atoms with different apex orientations (*e.g.* Figure 4).

The favored model has S−S distances of 5.34(3) Å and O(4)−O(4) distances ranging from 4.38(5) to 5.43(4) Å. Alternatively (Figure 4), Me_3SO^+ molecules occur in side-by-side ditrigonal rings but alternate between Me_3SO^+ planes [*e.g.* S−S = 6.10(3) Å, O(4)−O(4) = 4.19(4)−4.30(4) Å]. The models involve one molecule per paired ring in either the same or opposite Me_3SO^+ planes. Thus, the Me_3SO^+ tetrahedron is 3.5 Å from the oxygen apex to the methyl group triad base, and the interlayer separation is 7.099 Å. Sufficient space is present for the occupation of two planes of Me_3SO^+ pillars with alternate occupancy of planes. Rejected models include cases where S−S and O(4)−O(4) distances are too short (*e.g.* where S−S occurs within a paired ring or where two Me_3SO^+ molecules occur in the same Me_3SO^+ plane but at side-by-side ditrigonal rings occurring in the same 2:1 layer).

Me_3SO^+ orientation. The S atom is the source of the positive charge, and it offsets the net negative charge on the 2:1 layer by locating itself, in projection, in the center of the ditrigonal ring of tetrahedra. The oxygen apex of the Me_3SO^+ tetrahedron is located on the central plane of the interlayer owing to electrostatic repulsions from the negatively charged and adjacent 2:1 layers on the margins of the interlayer. In Me_3SO^+ tetraphenyl-borate, Knop *et al.* (1994) found that the Me_3SO^+ orientation is related to lone pairs of electrons on the oxygen atom of the structure and the interaction between the Me_3SO^+ cation and phenyl groups. Likewise, the lone pairs on the oxygen atom in exchanged vermiculite may also affect the Me_3SO^+ orientation relative to the 2:1 layer structure because the oxygen apex of the Me_3SO^+ tetrahedron is located at the center plane of the interlayer. The oxygen atom is probably pointing, in projection, directly toward one of the six tetrahedral sites (Figure 5), presumably if occupied by Si^{4+} and not Al^{3+}.

The refined location of sulfur is an average position with an apparent high thermal displacement parameter (Table 1). This large B value of 11.13 $Å^2$ is explained by positional disorder of the S in response to its bond to the Me_3SO^+ oxygen. Because the oxygen atom is located in any one of six positions (pointing toward the tetrahedral sites) surrounding the sulfur, the sulfur position shifts slightly to accommodate the location of the oxygen.

Methyl-group orientation. The methyl-group orientation is determined from the S−O(4) axis orientation and charge requirements of the bridging oxygen atoms of the tetrahedra, because electron-density maps were unsuccessful in locating either C or H. The substitution of Al

Table 5. Select distances relating possible Me_3SO^+ sites.

Two Me_3SO^+ sites occupying:	S−S (Å)	O4−O4 (Å)
Same set of paired rings and opposite Me_3SO^+ planes	2.95(3)	0.056(3)−1.50(4)
Side-by-side ditrigonal rings in the same 2:1 layer and the same Me_3SO^+ plane	5.34(3)	4.38(5)−5.43(4)
Side-by-side ditrigonal rings but alternating between Me_3SO^+ planes	6.10(3)	4.19(4)−4.30(4)

https://doi.org/10.1346/CCMN.2013.0610305 Published online by Cambridge University Press

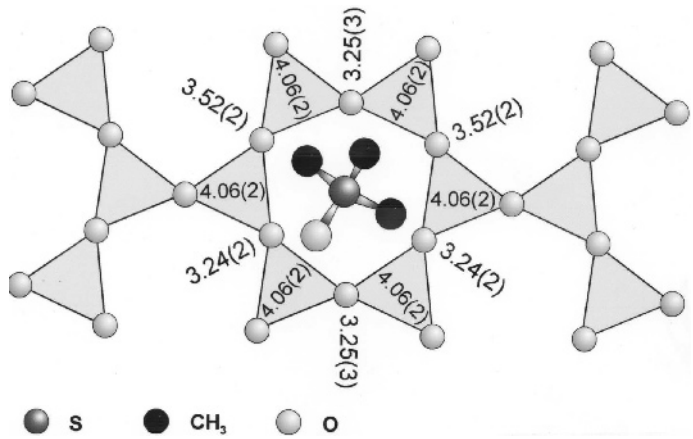

Figure 5. Sulfur-atom distance to the nearest tetrahedral plane of the adjacent 2:1 layer. Sulfur-atom to bridging-oxygen distances and sulfur atom to tetrahedral-cation distances (all distances as Å) are given. As noted in Figure 4, numbers in parentheses indicate estimated standard deviation, the projection is down the [001]* direction, and the 2:1 layer is incomplete.

in a tetrahedral site produces a positive charge deficiency of the associated bridging oxygen atom relative to Si, and a resulting attraction of the organic cation to the bridging oxygen atom. Covalent bonds were suggested by Loudon (1995) as possibly acting to enhance electrostatic effects; he considered the ionic character between atoms and the shared electrons of the covalent bond. For example, an oxygen atom can attract electrons from a covalent bond toward itself and, thus, is assigned a delta negative charge distribution. Equally, carbon atoms tend to repulse electrons from covalent bonds and are assigned a delta positive charge distribution. In Me_3SO^+, the methyl groups have a delta positive charge, and thus, satisfy the electrostatic character of the lone pair of the oxygen atom. Furthermore, the delta positive charge on the methyl groups will also aid in charge compensation of the charge-deficient bridging oxygen atoms in the tetrahedral sheets, and thus methyl groups may associate with these bridging oxygen atoms (Figure 6).

Santa Olalla vermiculite has a Si:^{IV}Al ratio of 5.48:2.52, or 1.33 Al ions per ditrigonal ring. The Me_3SO^+ molecules occupy 58% of the paired ditrigonal rings, and $\leqslant$66% of the rings may contain at least two Al. Where ditrigonal rings contain at least two tetrahedra occupied by Al, these tetrahedra are separated by at least one Si-tetrahedron (Loewenstein, 1954). Thus, ditrigonal rings may contain two Al substitutions (Figure 7). Although many combinations are possible for the locations of Al and Si, Figure 7 shows an arrangement to illustrate how the organic cation probably associates with the tetrahedral ring.

The tilt of the S–O(4) axis orients two methyl groups to point toward charge-deficient bridging oxygen atoms (note the arrows in Figure 7). Where a methyl group points toward a bridging oxygen atom of the tetrahedral sheet, the distance between a methyl hydrogen and the oxygen atom is ~1.84–2.45 Å, taken from the simulation models from the present study, and this may suggest that electrostatic interactions are occurring between the

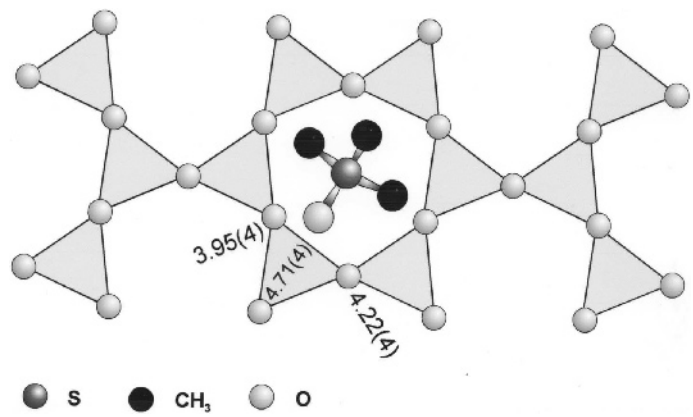

Figure 6. Distances (Å) of the oxygen atoms of the Me_3SO^+ molecule to bridging oxygen atoms of an associated tetrahedral cation site. See Figure 5 for information about the projection.

https://doi.org/10.1346/CCMN.2013.0610305 Published online by Cambridge University Press

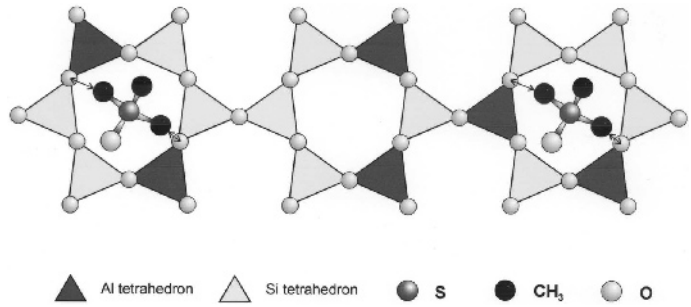

Figure 7. Several examples of Al substitution in the tetrahedral sheet. Each ring, on average, contains two Al atoms separated by at least one Si-bearing tetrahedron. Arrows indicate charge-deficient bridging-oxygen atoms closest to the methyl groups. See Figure 5 for information about the projection.

methyl hydrogen atoms and the bridging-oxygen atoms. When the methyl group is very close to the tetrahedral ring, the octahedral OH group tilts from its standard orientation perpendicular to the 001 plane, due to the repulsive interactions between the H atoms of the methyl and OH groups. The third methyl group is, thus, oriented in the interlayer as shown (Figure 7).

CONCLUSIONS

Organic pillars must charge compensate the bridging oxygen atoms of the 2:1 layer that are deficient in positive charge. Such charge deficiencies may occur either by tetrahedral substitutions, as commonly found in vermiculite, or by other substitutions elsewhere in the 2:1 layer. However, pillars with charge asymmetry, such as the Me_3SO^+ molecule, are required to position themselves such that the negative side of the molecule remains as far away from the 2:1 layer, an additional source of negative charge, as possible. To achieve this, the negative side of the molecule will align so that it resides midway between adjacent 2:1 layers.

In Me_3SO^+-exchanged vermiculite, the position of the Me_3SO^+ molecule is believed to be further stabilized by two methyl groups that can associate with bridging basal oxygen atoms of the ditrigonal silicate ring. Arguments involving lone pairs of electrons interacting within the Me_3SO^+ molecule suggest an electrostatic interaction between the methyl groups of the molecule and associated bridging basal oxygen atoms, rather than by hydrogen bonding. Thus, the ditrigonal aspects of the silicate rings that allow the approach of the methyl groups to the bridging basal oxygen atoms may, in part, be responsible for the alignment of the molecule where two methyl groups associate with the ditrigonal ring rather than an alternate arrangement where three methyl groups of the Me_3SO^+ tetrahedron might align with the ditrigonal ring. That the oxygen atom of the Me_3SO^+ molecule can position itself over a Si-containing tetrahedron may be further evidence of the veracity of the model presented here. The X-ray data suggest that H_2O molecules, if present, must be distributed randomly in the interlayer. The computer modeling confirms this conclusion.

If the asymmetry of charge distribution on the Me_3SO^+ molecule is influenced significantly by unshared electrons, the pillar may be a unique site for interlayer reactions. In addition, the attraction of the Me_3SO^+ molecule for fixing other molecules in the interlayer, such as environmental pollutants, may be enhanced by the effects of the unshared electrons.

ACKNOWLEDGMENTS

Dr A. Vahedi-Faridi is acknowledged and thanked for suggesting the project. The donors of The Petroleum Research Fund, administered by the American Chemical Society, are acknowledged for partial support of this research under grant PRF-32858-AC5. The U.S. National Science Foundation is acknowledged for support under grant EAR-0001122; the Junta de Andalucía is acknowledged for partial support under grant RNM-3581 CADHYS project; and the computational facilities of the Supercomputational Center of Granada University (UGRGRID) and Computing Center of CSIC are acknowledged also for support.

REFERENCES

Barrer, R.M. (1984) Sorption and molecular sieve properties of clays and their importance as catalysts. *Philosophical Transactions of the Royal Society of London*, **A311**, 333–352.

Barrer, R.M. (1989) Shape selective sorbents based on clay minerals: A review. *Clays and Clay Minerals*, **37**, 385–395.

Barrer, R.M. and Millington, A.D. (1967) Sorption and intracrystalline porosity in organo-clays. *Journal of Colloid Interface Science*, **25**, 359–372.

Barrer, R.M. and Perry, G.S. (1961) Sorption of mixtures, and selectivity in alkylammonium montmorillonites. *Journal of the Chemical Society*, 842–858.

Frisch, M.J., Trucks, G.W., Schlegel, H.B., Scuseria, G.E., Robb, M.A., Chesseman, J.R., Zarzewki, V.G., Montgomery, J.A., Stratmann, R.E., Burant, J.C., Dapprich, S., Millam, J.M., Daniels, A.D., Kudin, K.N., Strain, M.C., Farkas, O., Tomasi, J., Barone, V., Cossi, M., Cammi, R., Mennucci, B., Pomelli, C., Adamo, C., Clifford, S., Ochterski, J., Petersson, G.A., Ayala, P.Y., Cui, Q., Morokuma, K., Malick, D.K., Rabuck, A.D., Raghavachari, K., Foresman, J.B., Cioslowski, J., Ortiz, J.V., Stefanov, B.B., Liu, G., Liashenko, A., Piskorz, P., Komaromi, I., Gomperts, R., Martin, R.L., Fox, D.J., Keith, T.A., Al-Laham, M.A., Peng, C.Y., Nanayakkara, A., Gonzalez, C., Challacombe, M., Gill, P.M.W., Johnson, B.G., Chen, W.,

https://doi.org/10.1346/CCMN.2013.0610305 Published online by Cambridge University Press

Wong, M.W., Andres, J.L., Head-Gordon, M., Replogle, E.S., and Pople, J.A. (2004) *Gaussian 03* (Revision A.1), Gaussian, Inc., Pittsburgh, Pennsylvania, USA.

Guggenheim, S. (2013) Glossary for clay science. Updated annually and can be down loaded at: http://www.clays.org/GLOSSARY/GlossIntro.html

Hernández-Laguna, A., Escamilla-Roa, E., Timón, V., Dove, M.T., and Sainz-Díaz, C.I. (2006) DFT study of the cation arrangements in the octahedral and tetrahedral sheets of dioctahedral 2:1 phyllosilicates. *Physics and Chemistry of Minerals*, **33**, 655–666.

International Tables for X-ray Crystallography (Volume 4: Revised and Supplementary Tables to Volumes 2 and 3) (1974) J.A. Ibers and W.C. Hamilton, editors. The Kynoch Press, Birmingham, England, pp. 71–147.

Knop, O., Cameron, S., Bakshi, P.K., Linden, A., and Roe, S.P. (1994) Crystal chemistry of tetraradial species. Part 5. Interaction between cation lone pairs and phenyl groups in tetraphenylborates: Crystal structures of Me_3S^+, Et_3S^+, Me_3SO^+, Ph_2I^+, and 1-azoniapropellane tetraphenylborates[1,2]. *Canadian Journal of Chemistry*, **72**, 1870–1881.

Kolinsky, C., Puget, R., de Braver, C., and Jannin, M. (1994) Structures of trimethyloxosulfonium salts VIII. New refinement of the perchlorate $(CH_3)_3SO^+.ClO_4^-$. *Acta Crystallographica*, Section C, 1514–1516.

Lee, J., Mortland, M.M., Chiou, C.T., Kile, D.E., and Boyd, S.A. (1990) Adsorption of benzene, toluene, and xylene by two tetramethylammonium-smectites having different charge densities. *Clays and Clay Minerals*, **38**, 113–120.

Loewenstein, W. (1954) The distribution of aluminum in the tetrahedra of silicates and aluminates. *American Mineralogist*, **39**, 92–96.

Loudon, G.M. (1995) *Organic Chemistry*, third edition. The Benjamin/Cummings Publishing Company, Inc., California, USA.

Martos-Villa, R., Guggenheim, S., and Sainz-Diaz, C.I. (2013) Interlayer water molecules in organocation-exchanged vermiculite and montmorillonite: A case study of tetramethylammonium. *American Mineralogist*, **98**, DOI: 10.2138/am.2013.4370.

Norrish, K. (1973) Factors in the weathering of mica to vermiculite. Pp. 417–432 in: *Proceedings of the International Clay Conference 1972* (J.M. Serratosa, editor). Division de Ciencias, CSIC, Madrid.

Perdew, J.P., Ruzsinszky, A., Csonka, G.I., Vydrov, O.A., Scuseria, G.E., Constantin, L., Zhou, X., and Burke, K. (2008) Restoring the density-gradient expansion for exchange in solids and surfaces. *Physical Review Letters*, **100**, 136406.

Ruiz-Conde, A., Ruiz-Amil, A., Perez-Rodriguez, J.L., Sanchez-Soto, P.J., and Aragan de la Cruz, F. (1997) Interaction of vermiculite with aliphatic amides (formamide, acetamide and propionamide): Formation and study of interstratified phases in the transformation of Mg- to NH_4-vermiculite. *Clays and Clay Minerals*, **45**, 311–326.

Sainz-Diaz, C.I., Palin, E.J., Hernández-Laguna, A., and Dove, M.T. (2003) Octahedral cation ordering of illite and smectite. Theoretical exchange potential determination and Monte Carlo simulations. *Physics and Chemistry of Minerals*, **30**, 382–392.

Sainz-Díaz, C.I., Escamilla, E., and Hernández-Laguna, A. (2005) Quantum mechanical calculations of trans-vacant and cis-vacant polymorphism in dioctahedral 2:1 phyllosilicates. *American Mineralogist*, **90**, 1827–1834.

Seidl, W. and Breu, J. (2005) Single crystal refinement of tetramethylammonium-hectorite. *Zeitschrift für Kristographie*, **220**, 169–176.

Soler, J.M., Artacho, E., Gale, J.D., García, A., Junquera, J., Ordejón, P., and Sánchez-Portal, D. (2002) The SIESTA method for ab-initio order-N materials simulation. *Journal of Physics: Condensed Matter*, **14**, 2745–2779.

Stout, G.H. and Jensen, L.H. (1968) *X-ray Structure Determination: A Practical Guide*. John Wiley and Sons, Inc., New Jersey, USA.

Troullier, N. and Martins, J.L. (1991) Efficient pseudopotentials for plane-wave calculations. *Physical Reviews B*, **43**, 1993–2006.

Vahedi-Faridi, A. and Guggenheim, S. (1997) Crystal structure of tetramethylammonium-exchanged vermiculite. *Clays and Clay Minerals*, **45**, 859–866.

Vahedi-Faridi, A. and Guggenheim, S. (1999a) Structural study of tetramethylphosphonium-exchanged vermiculite. *Clays and Clay Minerals*, **47**, 219–225.

Vahedi-Faridi, A. and Guggenheim, S. (1999b) Structural study of monomethylammonium and dimethylammonium-exchanged vermiculites. *Clays and Clay Minerals*, **47**, 338–347.

(*Received 25 February 2013; revised 26 April 2013; Ms. 744; AE: H. He*)